Improvement of the Transmission Bandwidth for Indoor Optical Wireless Communication Systems Using a Diffused Gaussian Beam

Dehao Wu, *Student Member, IEEE,* Zabih Ghassemlooy, *Senior Member, IEEE,* Hoa Le Minh, *Member, IEEE,* Sujan Rajbhandari, *Member, IEEE,* and Anthony C. Boucouvalas, *Fellow, IEEE*

***Abstract*—The multipath dispersion in a non-directed line-of-sight (LOS) indoor optical wireless communications (OWC) channel limits the transmission bandwidth. In this study, we improve the transmission bandwidth by employing a TEM_{00} mode laser beam and an alignment-free light shaping diffuser (LSD). We derive a new expression for the radiation field distribution of the diffused Gaussian beam (DGB) and its multipath impulse response. The transmission bandwidth is determined based on the numerical simulation of the root mean square (RMS) delay spread in a room. Results show that indoor OWC systems employing DGB offers significantly higher transmission bandwidth compared to the Lambertian beam (LB) for a wide divergence angle.**

***Index Terms*—Optical wireless communications, diffused Gaussian beam, multipath dispersion and RMS delay spread.**

I. Introduction

OPTICAL wireless communications (OWC) for indoor applications has gone through a rapid period of research and development in the last decade [1], [2]. Compared with the traditional radio frequency (RF) technology and millimeter-wave systems, OWC systems offer a number of unique advantages including a large unlicensed bandwidth (hundred and thousand times higher than RF), immunity to electromagnetic interference, and a excellent security. With the increasing popularity of high definition television and video over the internet, the OWC indoor access technology becomes one of possible and economical solutions to address the bandwidth congestion currently experiencing in access networks [3].

There are two basic link configuration schemes for indoor OWC systems: a) the LOS and b) the diffused. The directed LOS optical link employing a very narrow divergence angle transmitter and a narrow field of view (FOV) receiver offers the minimum path loss and higher data rates; however at the cost of limited mobility and stringent link alignment. On the other hand, the diffused link provides an excellent mobility but suffers from the high path loss and multipath dispersion, which ultimately leads to the transmission bandwidth limitation. Non-directed LOS links employing wide-angle transmitters and receivers are more convenient to use, particularly for mobile terminals. In previous studies, practical error free indoor OWC systems up to 12.5 Gb/s have been demonstrated in a directed LOS link [4], [5]. However, little attention has been given to the non-directed LOS links with large coverage area necessary for indoor OWC applications, where the reflectivity from walls and ceiling cannot be ignored. There are a number of studies carried out on multipath dispersion characteristics of indoor OWC channels for diffused systems [6], [7], [8]. In all studies the Lambertian light source has been adopted; therefore overlooking the optimization of transmitter characteristics in terms of the radiation pattern. In this letter, we propose the DGB profile with a wide optical footprint as an alternative to Lambertian source and compare the performance of both systems in terms of the RMS delay spread D_{rms} for the non-directed LOS configuration. We also derive a new expression for the radiation field distribution for DGB. With the availability of cheap and alignment-free LSD [9], DGB based systems can provide a wide coverage area.

The rest of the paper is organized as follow. In section II, characteristics of both Gaussian beam and Lambertian beam are described. In section III, the simulation set up is outlined followed by results and discussion. Finally, the conclusion is given in the last section IV.

II. Channel Characteristics

A. Gaussian Beam with a LSD

The emitted beam of a single mode laser diode (LD) can be assumed as a spherical wave given by a point source. The irradiance distribution of the fundamental Gaussian TEM_{00} laser beam at distance L is given by [10]:

$$I(r,L) = I_0 \exp(-\frac{2r^2}{\omega^2(L)}) = \frac{2P}{\pi\omega^2(L)} \exp(-\frac{2r^2}{\omega^2(L)}), \quad (1)$$

where I_0 is the axial intensity, P is the total optical power of the beam,$r^2 = x^2 + y^2$ is the position at the terminal plane, and function $\omega(L)$ describes the evolution of the optical beam along the propagation direction L given by [10]:

$$\omega(L) = \omega_0[1 + (\frac{\lambda L}{\pi\omega_o^2})^2]^{0.5}, \quad (2)$$

where λ is the wavelength of light, ω_0 is the spot size radius (i.e. the radius where the field amplitude value drops to e^{-1} of the centre value) at the propagation distance $L = 0$. From(1) we can perceive that the irradiance intensity, at a given point, is dependent only on the beam waist radius $\omega(L)$. For a non-directed link covering a much wider area, the laser beam

Manuscript received April 12, 2012. The associate editor coordinating the review of this letter and approving it for publication was M. Leeson.

D. Wu, Z. Ghassemlooy, H. L. Minh, and S. Rajbhandari are with the Optical Communications Research Group, School of CEIS, Northumbria University, Newcastle upon Tyne, NE1 8ST, U.K. (e-mail: {dehao.wu, z.ghassemlooy, hoa.le-minh, sujan.rajbhandari}@northumbria.ac.uk).

A. C. Boucouvalas is with the University of Peloponnese, Department of Telecommunications Science and Technology, Tripolis, Greece (e-mail: acb@uop.gr).

This work is supported by EU FP7 Cost Actions of 1101.

Digital Object Identifier 10.1109/LCOMM.2012.060812.120803

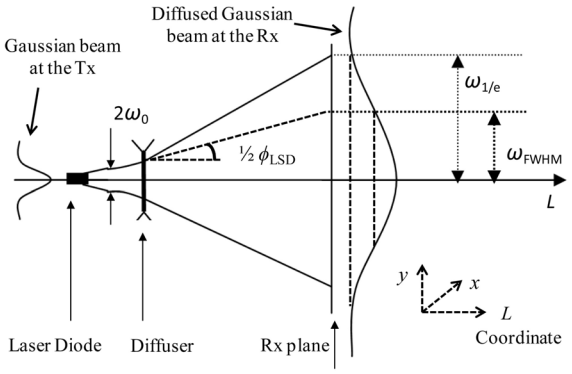

Fig. 1. Gaussian beam propagation through a diffuser.

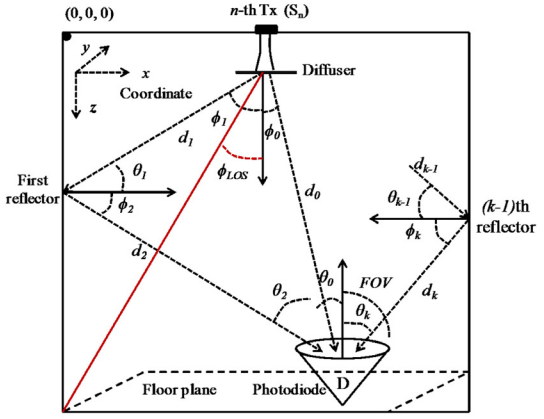

Fig. 2. Gaussian beam propagation through a diffuser.

should be passed through an optical diffuser as shown in Fig. 1. By doing so the beam waist radius will enlarge with a diffused angle $\phi_{diff}(L)$, which is given by [9]:

$$\phi_{diff}(L) \approx \sqrt{\phi_{div}^2(L) + \phi_{LSD}^2}, \tag{3}$$

where $\phi_{div}(L)$ is the full width at half maximum (FWHM) divergence angle of the laser diode (LD) and ϕ_{LSD} is the FWHM angle of LSD. Assuming the divergence angle of the LD is very small, i.e. $\phi_{div}(L) \ll \phi_{LSD}$, the diffused beam waist radius based on FWHM angle is given by:

$$\omega_{FWHM}(L) = L \tan \frac{1}{2}\phi_{LSD}, \tag{4}$$

As it is shown in Fig. 1, the beam waist radii based on FWHM angle and $\frac{1}{e}$ maximum angle $\omega_{\frac{1}{e}}(L)$ are different. To calculate the irradiance distribution of DGB with a diffused FWHM angle, we need to convert the beam waist radius of FWHM angle to the one of full width at $\frac{1}{e}$ maximum angle$\omega_{\frac{1}{e}}(L)$. From (1), we have:

$$I(0, L) = 2I[\omega_{FWHM}(L), L], \tag{5}$$

From (1), (4) and (5), $\omega_{\frac{1}{e}}(L)$is given by:

$$\omega_{\frac{1}{e}}(L) = \sqrt{\frac{2}{\ln(2)}}\omega_{FWHM}(L), \tag{6}$$

Therefore, for a diffused FWHM angle ϕ_{LSD}, the extended irradiance distribution of DGB is given by:

$$I(r, L) = I_0 \exp(-\frac{\ln(2)r^2}{L^2 \tan^2(\frac{1}{2}\phi_{LSD})}). \tag{7}$$

B. Lambertian beam

For the basic optical source like LED; the radiation pattern is modeled as Lambertian distribution, and the radiation distribution via LOS at the horizontal plane is give by [1]:

$$I(\phi) = \frac{m+1}{2\pi d^2} P \cos^m(\phi) \cos(\theta), \tag{8}$$

where m is the Lambertain order of radiation,ϕ is irradiance angle, θ is incidence angle, and d is the transmission distance between source and receiver. For a given half power angle $\phi_{\frac{1}{2}}$, the Lambertian radiant order is $m = -\frac{\ln(2)}{\ln(\cos(\phi_{\frac{1}{2}}))}$.

C. Multipath characteristics

In a non-directed indoor OWC system, the multipath-induced dispersion will limit the transmission data rate. A typical geometry of the link configuration of the non-directed LOS indoor OWC system is shown in Fig. 2. Depending upon the divergence angle of transmitter and receiver positions, the optical power after first reflection cannot be neglected. The optical power distribution and the multipath dispersion at the receiver plane can be characterized by the channel impulse response $h(t)$.

For a LOS channel, the irradiance distribution of a source using a generalized DGB radiation pattern having a uni-axial symmetry as in (1) and (7) is given by:

$$T(x, y, L) = \frac{\ln(2)P}{\pi L^2 tan^2(\frac{1}{2}\phi_{LSD})} \exp(-\frac{\ln(2)(x^2+y^2)}{L^2 tan^2(\frac{1}{2}\phi_{LSD})}), \tag{9}$$

The LOS impulse response for a particular source S and a detector $D(x, y, L)$, is given by [6]:

$$h^0(t; S, D) = \frac{T(x, y, L)}{P} A_R \cos(\theta_0) rect(\frac{\theta_0}{FOV})\delta(t - \frac{d_0}{c}), \tag{10}$$

where A_R is the physical surface area of detector,θ_0 is the LOS incidence angle, FOV is the field of view of the detector, d_0 is the LOS distance between S and D and c is the speed of light (see Fig. 2). The rectangular function $rect(x)$ is given by:

$$rect(x) = \begin{cases} 1 & \text{if } |x| \le 1; \\ 0 & \text{if } |x| > 1. \end{cases}$$

Assuming that all reflectors (i.e. plaster and acoustic-tiled walls, unvarnished wood) are approximately Lambertian [1], the channel impulse response with multiple optical sources and multiple reflections is given by [7]:

$$h^0(t; S, D) = \sum_{n=1}^{N_{source}} \sum_{k=0}^{\infty} h_n^k(t; S, D). \tag{11}$$

The channel response for exactly k-bounce with the extension for DGB pattern is given by [7]:

$$h^k(t; S, D) = \int_{\Psi} [\xi_0 \xi_1 ... \xi_k \rho^k rect(\frac{\theta_k}{FOV}) \delta(t - (\frac{\sum_{k=0}^{\infty} d_k}{c}))] dA_{ref}, k \ge 1 \tag{12}$$

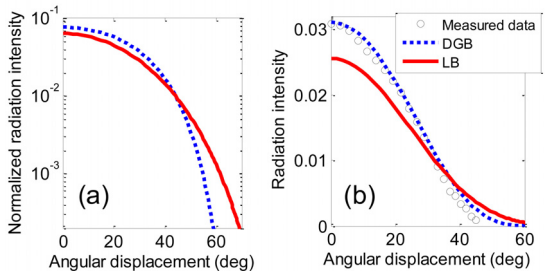

Fig. 3. Radiation intensity at horizontal plane: a) total optical power normalized to 1 W and L=3 m, b) total power normalized to 0.446 mW.

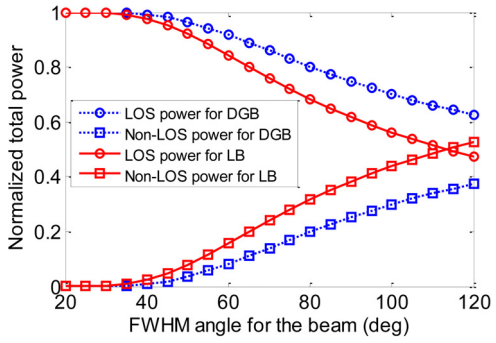

Fig. 4. The normalized total received power from LOS and diffused paths for LB and DGB sources.

where

$$\xi_0 = \frac{T(x,y,L)}{P} dA_{ref} \cos\theta_1,$$
$$\xi_1 = \frac{dA_{ref} \cos\phi_2 \cos\theta_2}{\pi d_2^2}, ...,$$
$$\xi_k = \frac{A_R \cos\phi_{k+1} \cos\theta_{k+1}}{\pi d_{k+1}^2}.$$

The integration in (12) is performed with respect to the surface Ψ of all reflectors, dA_{ref} is the small area of the reflecting element,ϕ_k and θ_k are the angles of irradiance and incidence, respectively, and d_k is the distance from k-bounce to the detector (see Fig. 2).

the RMS delay spread can be calculated using the impulse response h(t) given by [6]:

$$D_{rms} = [\frac{\int (t-\mu)^2 h^2(t) dt}{\int h^2(t) dt}]^{\frac{1}{2}}, \quad (13)$$

where t is the delay time of propagation and the mean delay μ is given by:

$$\mu = \frac{\int t h^2(t) dt}{\int h^2(t) dt} \quad (14)$$

III. Results and Discussion

The transversal intensity profiles of the DGB and LB against the angular displacement at L= 3 m for the normalized optical launch power of 1 W is given in Fig. 3. Both DGB and LB have a FWHM value of 80^o at a spherical plane, which corresponds to 56^o at the horizontal receiver plane with a vertical distance L of 3 m. The experimental results in Fig. 3(b) are carried out in a typical room environment

TABLE I
Specification for Indoor Non-directed LOS OWC System

Transmitter work wavelength (λ)	(500 ~ 1000nm)
Transmitter location	(2.5 m,2.5 m,0 m)
Transmitter beam radius (ω_0)	(0.1mm)
Transmitter diffused angle (ϕ_{LSD})	120^o
Receiver location	(0.5 m,1.0 m,3.0 m)
Half angle FOV of photodiode	60^o
Surface area of photodiode photodiode	$1cm^2$
Reflection coefficient of wall, ceiling and floor	(0.8, 0.8, 0.3)

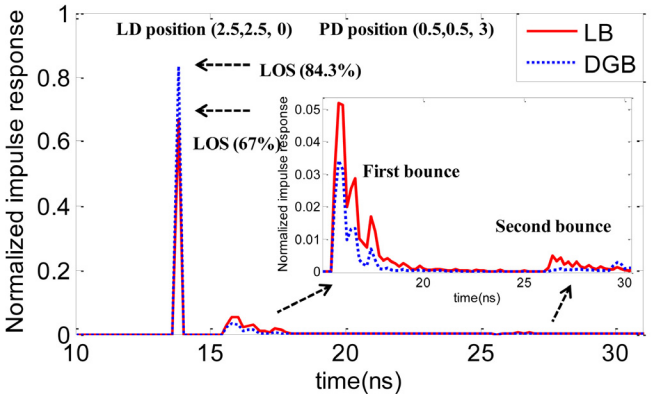

Fig. 5. The normalized impulse response of DGB and LB for the LOS link and first reflection.

using Luminit 80^0 (spherical FWHM angle) LSD and the Heliumneon (HeNe) laser with a wavelength of 543.5 nm. The irradiance distribution for DGB is wavelength independent and the selection of visible wavelength at 543.5 nm is purely for easy alignment. Based on the measured total power of LD is 0.45 mW, the normalized theoretical radiation intensity is plotted in Fig. 3(b). The intensity profiles of DGB and LED under the same conditions are also shown for comparison. The results illustrate that the DGB pattern has a sharper tail than LB.

In order to carry out a comparative study of DGB and LB sources, the impulse response and the RMS delay spread are determined by means of numerical simulation for a typical room with a dimension of $5 \times 5 \times 3m^3$ (length, width, height) with the optical source and receiver located at the ceiling and the floor level, respectively (see Fig. 2). The total normalized received optical power in the receiver plane received via the LOS path P_{LOS} and the diffused path P_{Non_LOS} for a range of FWHM angles is illustrated in Fig. 4. As the FWHM angle increases the P_{LOS}decreases for both DGB and LB, while P_{Non_LOS} increases. The comparative study shows that $P_{Non_LOS}$from DGB is less than that of LB for the same divergence angle condition and the difference increase as the FWHM angle increases.

The normalized received optical power gives an indication that for a given FWHM the dispersion is less severe in DGB. In order to quantify the performance gain achieved from using DGB, we calculate the RMS delay spread and the transmission bandwidth of a non-directed LOS link with the parameters specified in Table I.

Using the approach adopted in [6], we simulate the mul-

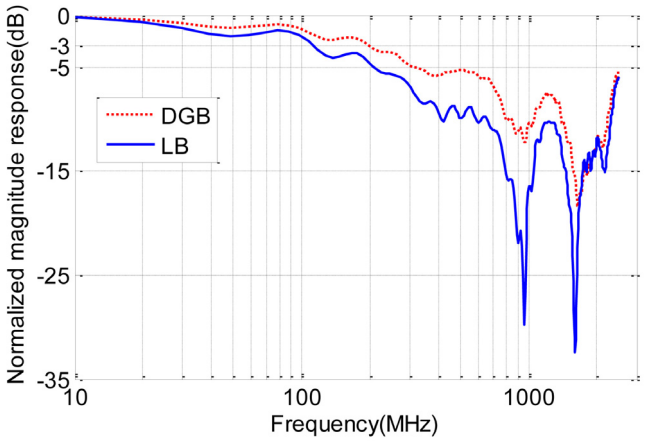

Fig. 6. The normalized magnitude frequency response of DGB and LB up to second bounce reflection.

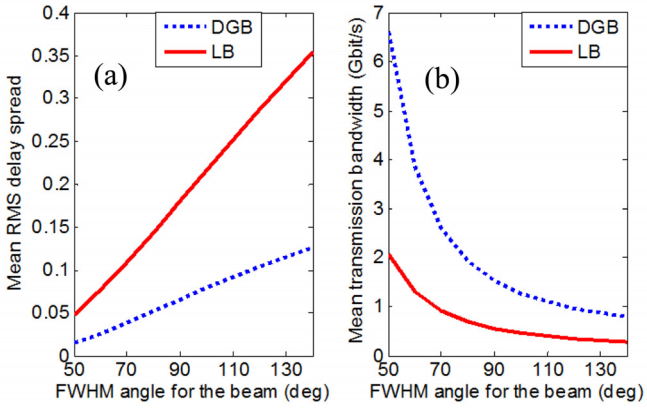

Fig. 7. RMS delay spread and maximum achievable data rate for the non-directed LOS indoor OWC link with LB and DGB sources.

tipath impulse response and the RMS delay spread for DGB and LB for the same FWHM divergence angle. The reflected power from the third bounce is very small, which is less than 3% in most configurations [6], [11], [12]. Fig. 5 depicts the normalized impulse response of the LOS link, and the first and second reflections. The amplitude of received signal from the second bounce is very low, which is less than 1% of LOS power as shown in Fig. 5. Since the received optical power for higher reflections are significantly low (less than 0.5%), the higher order reflections (third bounce or more) is not considered in this study. The amplitude of received power from the LOS link for DGB is 0.84, which is 17.3% higher than the LOS received signal from LB. However, the amplitude of received signal from the first and second reflections is higher in LB. To highlight the effects of higher-order bounces on the 3-dB bandwidth, the frequency response of the system is given in Fig. 6. It can clearly be seen from the figure that DGB offers higher 3-dB bandwidth in comparisons with the LB.

In order quantify the multipath dispersion of the proposed model; the average RMS delay spreads as well as the maximum achievable data rate for a non-directed LOS channel for both DGB and LB with different FWHM angles are shown in Figs. 7(a) and (b). It can clearly be seen that DGB has the lower mean RMS delay spread compared with the LB. The maximum bit rate, which can be transmitted through the indoor channel, is calculated following [13]: $R_b \leq \frac{1}{10D_{rms}}$. The results in Fig. 7 show that, for a wide divergence angle, the DGB model has lower non-LOS channel mean RMS delay, which is around half of the LB model and hence doubling the maximum transmission bandwidth.

IV. Conclusion

A DGB has been proposed in order to improve the transmission rate of non-directed LOS indoor OWC systems. A new expression for the radiation field distribution of DGB is derived and the multipath impulse responses were calculated. Multipath dispersion is estimated by quantifying the RMS delay spread. Compared with the traditional LB OWC model, the DGB model with the appropriate divergence angle significantly improves the indoor transmission bandwidth.

References

[1] M. Kavehrad and S. Jivkova, "Indoor broadband optical wireless communications: optical subsystems designs and their impact on channel characteristics," *IEEE Wireless Commun.*, vol. 10, no. 2, pp. 30–35, Apr. 2003.

[2] R. Green, H. Joshi, M. Higgins, and M. Leeson, "Recent developments in indoor optical wireless [optical wireless communications]," *IET Commun.*, vol. 2, no. 1, pp. 3–10, Jan. 2008.

[3] D. O'Brien, G. Parry, and P. Stavrinou, "Optical hotspots speed up wireless communication," *Nature Photonics*, vol. 1, no. 5, pp. 245–247, 2007.

[4] K. Wang, A. Nirmalathas, C. Lim, and E. Skafidas, "High-speed optical wireless communication system for indoor applications," *IEEE Photonics Technol. Lett.*, vol. 23, no. 8, pp. 519–521, Apr. 15, 2011.

[5] H. L. Minh, D. O'Brien, G. Faulkner, O. Bouchet, M. Wolf, L. Grobe, and J. Li, "A 1.25-gb/s indoor cellular optical wireless communications demonstrator," *IEEE Photonics Technol. Lett.*, vol. 22, no. 21, pp. 1598–1600, Nov. 1, 2010.

[6] J. B. Carruthers and S. M. Carroll, "Statistical impulse response models for indoor optical wireless channels," *Int'l J. Commun. Syst.*, vol. 18, no. 3, pp. 267–284, 2005.

[7] K. Lee, H. Park, and J. Barry, "Indoor channel characteristics for visible light communications," *IEEE Commun. Lett.*, vol. 15, no. 2, pp. 217–219, Feb. 2011.

[8] A. G. Al-Ghamdi and J. M. H. Elmirghani, "Multiple spot diffusing geometries for indoor optical wireless communication systems," *Int'l J. Commun. Syst.*, vol. 16, no. 10, pp. 909–922, 2006.

[9] Luminit, "Light shaping diffuser datasheet," 2012.

[10] P. Goldsmith, *Gaussian Beam Quasioptical Propogation and Applications*, 1998.

[11] T. Komine and M. Nakagawa, "Fundamental analysis for visible-light communication system using LED lights," *IEEE Trans. Consum. Electron.*, vol. 50, no. 1, pp. 100–107, 2004.

[12] A. G. Al-Ghamdi and J. M. H. Elmirghani, "Spot diffusing technique and angle diversity performance for high speed indoor diffuse infra-red wireless transmission," *IEE Proc.-Optoelectronics*, vol. 151, no. 1, pp. 46–52, 2004.

[13] T. S. Rappaport, *Wireless Communications*, 2002.